GL-TR-89-0337

AD-A216 325

A STUDY OF THE EVOLUTION OF SOLAR ACTIVE REGIONS
FOR IMPROVING SOLAR FLARE FORECASTS

Patricia L. Bornmann
Cooperative Institute for Research in Environmental Sciences
NOAA Space Environment Laboratory
325 Broadway, R/E/SE
Boulder, CO 80303 USA

and

Darren Kalmbach, David Kulhanek, and April Casale
Computer Science Department
University of Colorado
Boulder, CO 80309 USA

DTIC
ELECTE
JAN 0 2 1990
B

ABSTRACT

Statistics on the frequency of transition between active region classes were calculated and used to derive the expected rate of flaring for the next 2–7 days. Five years of McIntosh active region classifications were analyzed using the newly-developed software called TELSAR (Tracking and EvoLution of Solar Active Regions). The most frequent transitions between these 63 different classes usually involve a single-step change in one of the three classification parameters. The evolution of the classes and the average, single-day flare rate were used to predict flare rates for each class over the next several days. For flares of X-ray class M (peak 1-8 Å flux between 10^{-5} and 10^{-4} W m^{-2}), these rates can differ from persistence predictions by more than 0.5 flares per day, although a more typical difference is 0.1 flares per day. The rarity of some classes suggests that merging these classes with others may improve flare statistics and thereby improve flare forecasts.

1. INTRODUCTION

Operational solar flare predictions are routinely made using the reported three-parameter McIntosh active region classes and the flare probability for each of these classes. A total solar flare forecast for each day is derived from the sum of the average number of flares for the class of each observed solar active region. Flare predictions for more than one day, however, require estimates of the evolution of the region and how much the flaring rate should change. At present these estimates rely on the forecaster's experience, because no evolutionary statistics were previously available. The present study provides these evolutionary statistics, and combines them with flare probabilities to give an expected flare probability for the next 2–7 days.

Although every solar active region exhibits different white light spatial characteristics, each can be assigned to a class, using the three-parameter extension (McIntosh 1981, 1989) to the original single-parameter Zürich sunspot classification (Kiepenheuer 1953, Waldmeier 1955). These three parameters, summarized in Figure 1, are based primarily on the region's magnetic configuration, degree of penumbral development, spatial scales, and spot distribution. The first parameter describes the nature of the group, the second parameter describes the degree of development of the largest spot in the group, and the third parameter describes the amount of spot development in the interior of the group. Together, these three parameters form a set of 63 allowable classes (Kildahl 1980), that can be used to examine the complexity and maturity of the region. We have listed these parameters from left to right and then top to bottom in the summary figure in rough order of increasing complexity. This is not a definitive ordering, and future analysis may suggest reordering these parameters.

Because of solar rotation, the entire evolution of a single solar active region is rarely observable. We assume that similarities of evolution occur, and that the evolution of each region is not totally random. This assumption is based on the evolutionary nature of the original single-parameter classification (Bray and Loughhead 1964). Therefore, by comparing the evolution of many regions, we can derive the probable evolution of a solar active region.
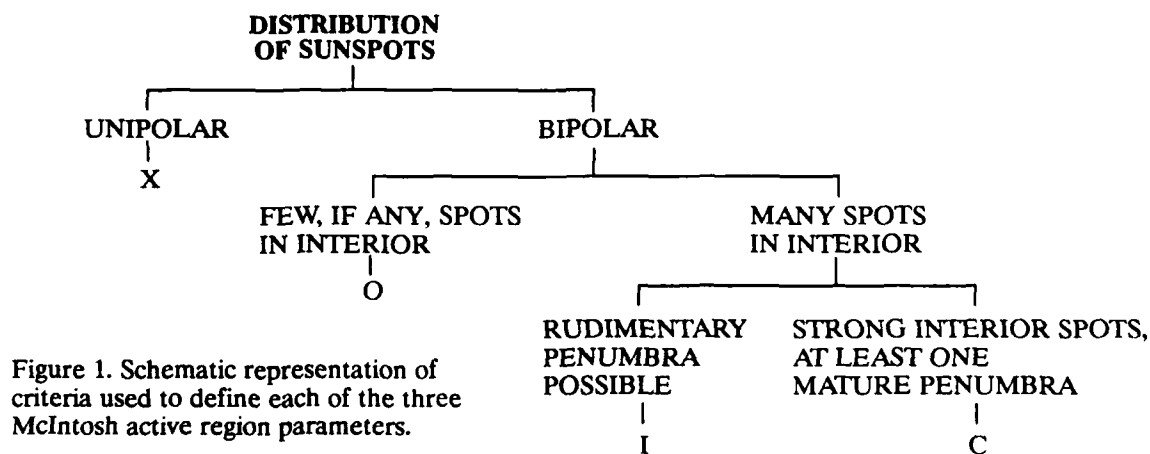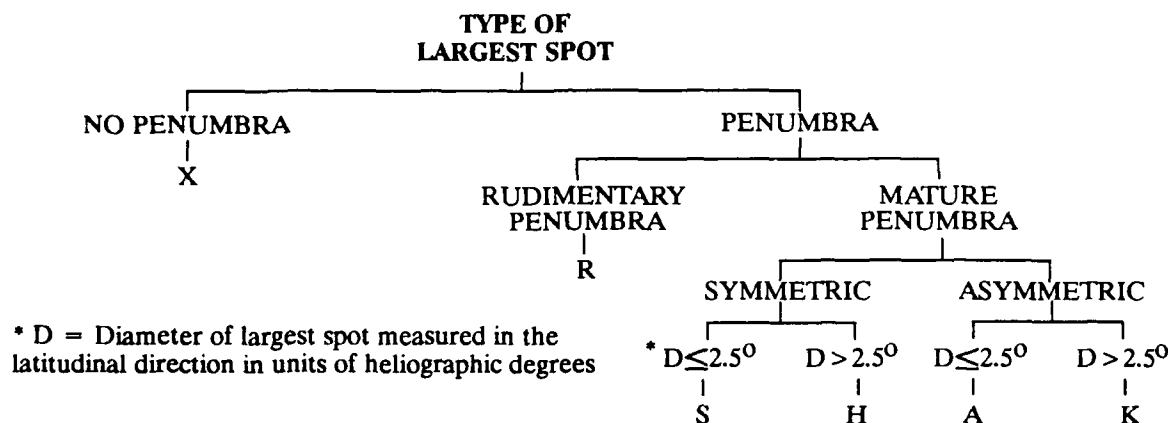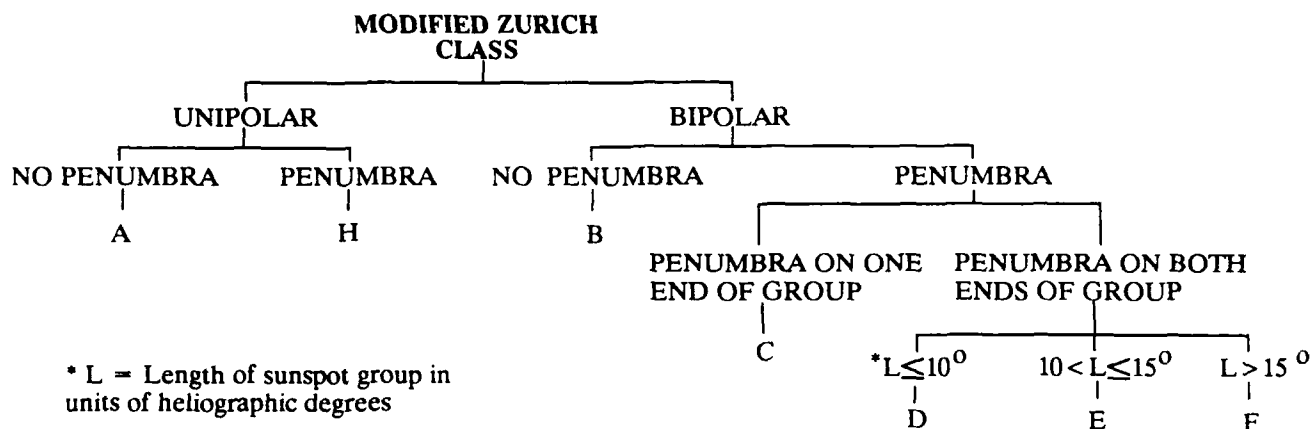
2. THE TELSAR ANALYSIS SOFTWARE

We have recently developed new software, called TELSAR for Tracking and EvoLution of Solar Active Regions, to calculate statistics on the evolution of active regions through the three-parameter classification system. For our analysis,

90 01 02 048

MODIFIED ZURICH CLASS

- **UNIPOLAR**
  - NO PENUMBRA — A
  - PENUMBRA — H
- **BIPOLAR**
  - NO PENUMBRA — B
  - PENUMBRA
    - PENUMBRA ON ONE END OF GROUP — C
    - PENUMBRA ON BOTH ENDS OF GROUP
      - $^{*}L \leq 10^{\circ}$ — D
      - $10 < L \leq 15^{\circ}$ — E
      - $L > 15^{\circ}$ — F

* L = Length of sunspot group in units of heliographic degrees

TYPE OF LARGEST SPOT

- **NO PENUMBRA** — X
- **PENUMBRA**
  - RUDIMENTARY PENUMBRA — R
  - MATURE PENUMBRA
    - SYMMETRIC
      - $^{*}D \leq 2.5^{\circ}$ — S
      - $D > 2.5^{\circ}$ — H
    - ASYMMETRIC
      - $D \leq 2.5^{\circ}$ — A
      - $D > 2.5^{\circ}$ — K

* D = Diameter of largest spot measured in the latitudinal direction in units of heliographic degrees

DISTRIBUTION OF SUNSPOTS

- **UNIPOLAR** — X
- **BIPOLAR**
  - FEW, IF ANY, SPOTS IN INTERIOR — O
  - MANY SPOTS IN INTERIOR
    - RUDIMENTARY PENUMBRA POSSIBLE — I
    - STRONG INTERIOR SPOTS, AT LEAST ONE MATURE PENUMBRA — C

Figure 1. Schematic representation of criteria used to define each of the three McIntosh active region parameters.

we have added two more classifications to examine the evolution from birth to death of a region. The birth class, YYY, was added if the region was first observed west of E70 deg. Similarly, a death class, ZZZ, was added if the last region report occurred before reaching W70 deg.

The reported active region classes for each region were converted into a separate evolutionary "tree" showing the evolution from one class to the next. These trees were then used to calculate evolutionary and flare statistics. The evolutionary statistics include the minimum, maximum, and average length of time for regions of one class to evolve into another class, and probability and total number of regions making these transitions. The flare statistics give the probable number of flares per day for each class after a specified number of days have elapsed.

Because a region was usually classified by a number of different observatories, the classifications for a given day may be inconsistent. TELSAR has two primary methods for dealing with these inconsistencies. The first method is an equal-weight vote from each of the reported classifications on that day. A tie vote is resolved using the reported reliability
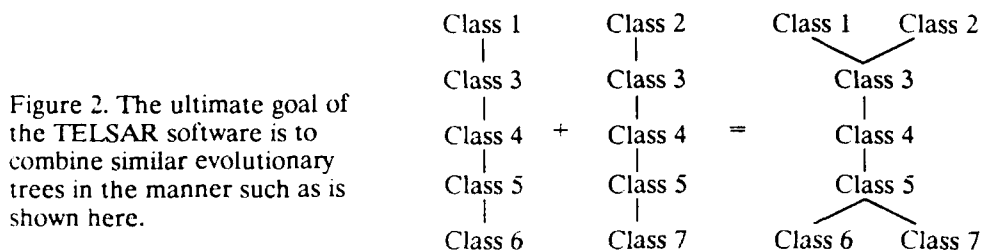
of the observations. The second method is a reliability-weighted average of each of the three classification parameters. Combinations of parameters that would give an illegal class are redefined according to an algorithm used by the SEL Space Environment Services Center (developed by J. Bryson and D. Snelling; C. Cruickshank 1988 private communication). We have used this second method, the SESC average, for all of the analysis presented in this paper.

TELSAR was designed to analyze subsets of the data based on different criteria. Data can be chosen based on a range of dates, range of region numbers, or evolution through a particular class. Less reliable data can be automatically discarded whenever the observatory-reported reliability lies below some limit. Data can also be discarded whenever the region was within a specified distance from the limb, where foreshortening makes the classification more difficult.

TELSAR can compare the evolutionary patterns of the separate trees and combine them when they have a sufficient number of similar transitions between classes. This is done in an effort to piece together the probable evolution of regions on the back side of the sun. The resulting combined trees (shown schematically in Figure 2) can then be analyzed to determine the statistical properties beyond the observational window.

Figure 2. The ultimate goal of the TELSAR software is to combine similar evolutionary trees in the manner such as is shown here.

Because TELSAR's ability to correctly combine evolutionary sequences is still being tested, this paper will concentrate on statistics derived without combining trees. Because no tree combining is performed, the evolution into the far future will not be considered. The evolution several days into the future should not be severely affected, since the observational window due to solar rotation is approximately 14 days.

3. DATA

The present analysis uses a subset of the active region classifications available on magnetic tape from the World Data Center. We have used the classifications from December 1981 through the end of 1986, which includes a total of 1158 active regions with identification numbers between 3477 and 4762. A total of 32,932 individual active region reports were examined, of which 32,705 contained useable, legal classifications (see section 4.3). The three-parameter active region classifications were assigned in real time at the U.S. Air Force Solar Observing Optical Network (SOON) sites for use in flare forecasting by the NOAA Space Environment Services Center and the USAF Global Weather Central. Up to eight different sites contributed their daily active region reports, which, after averaging all reports for the same region and day, gave a total of 7030 region classifications. Therefore, an average of 4.7 daily reports were combined to form an average sequence of 6.1 days of classifications. We have chosen not to analyze the early 10 years of data at this time, in part because many of the SOON sites were not yet operational.

4. RESULTS

4.1 TRANSITIONS BETWEEN CLASSES

In Table 1 we present the statistics on the number of direct transitions between classes. This table is a 65x65 array listing the scaled number of regions that evolved from the class listed in the left hand side into the class listed at the top. We have ordered the classes from the left to right and then top to bottom as shown in Figure 1. Appended to the end of this class sequence are our birth and death classes. Each class was assigned a class number, given in parenthesis. These same two-digit class numbers are repeated at the top of the table, and should be top to bottom.

In order to conserve space, we have scaled the number of direct transitions between SESC-averaged classes and rounded this scaling to a integer. We use a logarithmic scaling, s, of the form

$$s = 10. * \log x / \log [max(x)]$$

where x is the number of regions observed to make a direct transition between classes. The scaled numbers run from 0 to 9 with a number sign "#" for the maximum of 10. The maximum number of transitions, max(x), was 431, so this scaling reduces to

Table 1. Scaled number of transitions 1981-1986

```
          0000000000011111111112222222222333333333344444444445555555555566666
          01234567890123456789012345678901234567890123456789012345678901234
AXX( 0)   .54.0.906150..4...3..40..0.4..1...........1...................#
HRX( 1)   7.4.0.6.3.4...1......1.....1.....................4
HSX( 2)   66.66.5.207.3.4.000..3..2..2..1.....0....1...0.................4
HHX( 3)   ..7.33....3.5.2.2....2..0..0..1.0.........0...........
HAX( 4)   2.52.02.1.4.2.3.0....0.....10.............0................2
HKX( 5)   ..131.....0...1.0.........00.110.....................
BXO( 6)   #5402...8171..5.0.40.62.20.52.00...........0.............9
BXI( 7)   ...........................10...............
CRO( 8)   642.0.8...7.2.2...30.51....52.01.................4
CRI( 9)   0........0...0..........00.............0............
CSO(10)   56843.706..05.6.103..73.30.62.10....2.....2..........0.........3
CSI(11)   .0....0.....0.......0...01.....................
CHO(12)   0.35200...60..4.3....0..2..3..01.........0..0..............0
CHI(13)   ...0...............0.........................
CAO(14)   42523.5.3.7040..3.0..40.1..53.020...0...2.............0...2
CAI(15)   ................0............................
CKO(16)   ..1110....0.3.30.0...0..0..2..101.................0
CKI(17)   ............0..1...........0..1.................
DRO(18)   30....4.3.2...0....0.20...3....................1
DRI(19)   .....0.0.........0...0...................
DRC(20)*  ....................................
DSO(21)   125.1.5.5.702.5.0.2...3.50.74.22....3..30.22.010.............2
DSI(22)   ........2.2...0......3..00.31.00..........02.00....0.........0
DSC(23)   ....................................
DHO(24)   ..20.00...3.402..0...3...3.42.22....0..00.0..00............2
DHI(25)   ..........1...........20.3...2.01.......0..0..2..........0...
DHC(26)   ....................................
DAO(27)   2020204.4.6.3.5...2..72.41..5.43....3..10.43.23...........0.0...3
DAI(28)   ........1.2...1.....33.03.5..14......0.0..24.13............00...
DAC(29)   ........0................................
DKO(30)   ..0.11....0.2.2.30...4..22.42..3........0....320.............
DKI(31)   0...00.........1......01.24.4.4........11.24...........0..0
DKC(32)   ............................14.........0............0...
ERO(33)   ................0..0......................
ERI(34)   ................0.........................
ERC(35)*  ....................................
ESO(36)   ..0...1.2.4...0.....30.0..2.........1....21.0.............
ESI(37)   .....0...0.........1.....0......0....2.0.............
ESC(38)*  ....................................
EHO(39)   ..0.......1.3...0....1.1..0........2...1.2..32..........0.........0
EHI(40)   .........0........00..0..0......3..20.0..............
EHC(41)   ....................................
EAO(42)   0.2.1.0.0.0.0.1.0.0..2..1..41....0..40.20..3.31............10..0...
EAI(43)   ..0.......0...0.....00.0..21..0....23.2..3...04.......0...0...0...
EAC(44)   ...................................0............
EKO(45)   0...1.....0.0.0000...0..0..1..31....2..3..4...20...........31...
EKI(46)   ....00......0.0.0....0..00..0.230...00.22.3304.3.........01..4...
EKC(47)   ......................0.............3........01..
FRO(48)   ....................................
FRI(49)*  ....................................
FRC(50)*  ....................................
FSO(51)   ......................0...............0........
FSI(52)   ...............................0.....
FSC(53)*  ....................................
FHO(54)   ...............0..0..0.........00............1......
FHI(55)   ...........................1...1..1...
FHC(56)   ....................................
FAO(57)   .........1.0.0.....0.......1.....0........1..0......
FAI(58)   ................0...........1.....0....1..02...
FAC(59)   ....................................
FKO(60)   .................0..0.0.........0..2........1.0...2...
FKI(61)   ...................0.0.........0.10.13........2.10.3.3..
FKC(62)   ....................0.............0........0..4...
YYY(63)   93400.90706.  4.0.10.40....520.0..0.....0.0..............0...
ZZZ(64)   ....................................
```

4

$$x = 1.83^S$$

and the scaled numbers from 0 to 4 correspond to approximately 1, 2, 3, 6, and 11 occurrences. In addition, a period "." is used to indicate transitions that did not occur, and an asterisk "*" notes the classes that did not occur in the original data.

A large number of transitions occurred between neighboring classes. For ~80% of the classes, the most likely next class is only one parameter different. And in these cases, the one parameter generally changed by only one step in the left-to-right progression of the flare parameters shown in Figure 1. The primary exception to this is the set of second parameters S, H, A, and K, which are based on combinations of the sunspot size and symmetry.

For one third of the classes, the most probable transition into and out of this class involved the same second class. This suggests the two possibilities illustrated in Figure 3. Either the reported classes are oscillating between neighboring classifications due to observational errors, or the sequence followed by growing regions is traversed in the opposite direction by decaying regions. These two possibilities can be tested using a running average of the classes with time. Such an average should reduce the number of oscillating classifications. Alternatively, the examination of individual or combined trees may reveal the answer. These tests have not yet been performed.

Class 2 $\longrightarrow$ Class 1 $\longrightarrow$ ..... $\longrightarrow$ Class 1 $\longrightarrow$ Class 2

Class 1 $\rightleftharpoons$ Class 2

Figure 3. Traversing the same transitions forwards and then backwards or oscillating between classes are two possible causes for the result that the most probable transitions into and out of a class often involve the same intermediate class.

4.2 FLARE PROBABILITIES

TELSAR calculates the rate of M flares per day expected to occur 2 to 7 days after the observed classification. These rates were derived using all observed active regions from December 1981 through 1986, without the combining indicated in Figure 2. For each class, TELSAR determined all classes that those regions evolved into after a specified number of days. This was then used along with the average number of flares, P_i, for these subsequent classes (Kildahl 1980) to calculate the expected flare rate for that day. (We used his table of class occurrences to resolve two typographical errors in the flare probability, which listed the flare probabilities for classes HRX and FRO listed twice, and omitted HHX and FKO.) Thus, this is not the actual number of flares observed for that region several days later, but a statistically predicted average. Finally, the expected flare rate, R, in units of M flares per day is derived from

$$R = \sum P_i N_i / \sum N_i$$

were N_i is the number of regions of class i observed on the specified day. We have included a zero average number of flares for the birth and death classes, but did not consider a region to contribute zero flares after the first day in the death class (ZZZ). This could affect the calculated flare rate, and cause an artificial rise for the day after the death class. However, since decaying regions do not produce many flares, this will not seriously alter the flare forecast. We also note that the confidence in this flare rate will decrease with time because the number of regions observed for long periods of time decreases due to solar rotation with the time interval.

In table 2 we list the calculated flare rates. The first column lists the classes, along with an asterisk for those classes that did not occur in the original data. The second column lists the average number of flares per day derived by Kildahl (1980) for the years 1969 to 1976. The remaining columns list the future flare rate R, with periods to indicate when no classes were observed on the specified future day.

Regions near the top of the table tend to be simple, and produce increasing numbers of flares with time. Regions near the bottom of the table are more complex and are likely to have a maximum flare rate within the next several days.

These evolutionary statistics are expected to provide better flare forecasts for the next several days than persistence forecasts. The presistence forecast does not consider evolution of the region or changes in the flare rate with time. This can be seen by comparing the same day flare rates in column two of Table 2 with the following columns. The maximum flare rate expected in the next several days can be up to a factor of 7 larger than for the current day, although a more typcial

Table 2. Average number of M flares per day

Class	per day	day 2	day 3	day 4	day 5	day 6	day 7
AXX(0)	0.01	0.02	0.03	0.04	0.06	0.08	0.07
HRX(1)	0.03	0.03	0.04	0.03	0.06	0.07	0.14
HSX(2)	0.05	0.06	0.06	0.07	0.08	0.09	0.11
HHX(3)	0.11	0.09	0.12	0.13	0.12	0.13	0.15
HAX(4)	0.06	0.06	0.11	0.11	0.12	0.11	0.08
HKX(5)	0.18	0.20	0.22	0.24	0.20	0.22	0.26
BXO(6)	0.02	0.03	0.03	0.04	0.06	0.08	0.09
BXI(7)	0.06	0.12	0.40	0.26	0.45	0.15	0.30
CRO(8)	0.05	0.04	0.05	0.06	0.08	0.08	0.10
CRI(9)	0.05	0.17	0.27	0.18	0.23	0.32	0.12
CSO(10)	0.04	0.06	0.06	0.06	0.07	0.07	0.09
CSI(11)	0.08	0.10	0.11	0.06	0.03	0.02	0.02
CHO(12)	0.07	0.09	0.12	0.14	0.13	0.13	0.12
CHI(13)	0.21	0.18	0.15	0.09	0.19	....	....
CAO(14)	0.08	0.08	0.09	0.12	0.12	0.12	0.11
CAI(15)	0.11	0.08	0.10	0.04	0.01	....	....
CKO(16)	0.25	0.16	0.19	0.15	0.14	0.15	0.12
CKI(17)	0.21	0.31	0.28	0.37	0.10	0.49	0.34
DRO(18)	0.08	0.05	0.04	0.07	0.04	0.03	0.04
DRI(19)	0.13	0.10	0.18	0.08	0.05	0.00	....
DRC(20)*	0.00	....	....	....	....	....	....
DSO(21)	0.09	0.10	0.12	0.12	0.14	0.16	0.17
DSI(22)	0.13	0.21	0.25	0.24	0.22	0.29	0.31
DSC(23)	0.25	....	....	....	....	....	....
DHO(24)	0.26	0.16	0.27	0.24	0.21	0.20	0.19
DHI(25)	0.07	0.48	0.37	0.36	0.41	0.35	0.18
DHC(26)	0.33	....	....	....	....	....	....
DAO(27)	0.10	0.14	0.16	0.17	0.17	0.16	0.17
DAI(28)	0.18	0.30	0.31	0.32	0.33	0.29	0.29
DAC(29)	0.26	0.08	0.08	0.10	0.10	0.08	0.08
DKO(30)	0.33	0.31	0.30	0.34	0.36	0.24	0.32
DKI(31)	0.48	0.49	0.53	0.46	0.49	0.45	0.46
DKC(32)	0.72	0.66	0.55	0.50	0.50	0.45	0.45
ERO(33)	0.00	0.09	0.05	0.11	0.10	0.08	0.08
ERI(34)	0.00	0.08	0.05	0.05	0.02	0.00	....
ERC(35)*	0.00	....	....	....	....	....	....
ESO(36)	0.17	0.18	0.13	0.17	0.13	0.18	0.22
ESI(37)	0.17	0.24	0.26	0.31	0.27	0.16	0.08
ESC(38)*	0.00	....	....	....	....	....	....
EHO(39)	0.15	0.26	0.38	0.34	0.34	0.29	0.42
EHI(40)	0.62	0.33	0.35	0.23	0.16	0.19	0.15
EHC(41)	2.00	....	....	....	....	....	....
EAO(42)	0.21	0.27	0.25	0.30	0.33	0.23	0.28
EAI(43)	0.58	0.58	0.53	0.51	0.47	0.48	0.43
EAC(44)	0.35	0.35	1.27	0.58	0.10	0.00	....
EKO(45)	0.38	0.40	0.50	0.43	0.36	0.44	0.51
EKI(46)	1.27	1.02	0.96	0.89	0.81	0.78	0.66
EKC(47)	2.37	2.07	1.71	1.50	1.16	1.09	1.16
FRO(48)	0.00	....	....	....	....	....	....
FRI(49)*	0.50	....	....	....	....	....	....
FRC(50)*	0.00	....	....	....	....	....	....
FSO(51)	0.46	0.23	0.40	0.27	0.10	0.36	0.10
FSI(52)	1.88	0.00	0.00	0.09	0.06	....	....
FSC(53)*	0.00	....	....	....	....	....	....
FHO(54)	0.00	0.14	0.09	0.21	0.29	0.16	0.23
FHI(55)	0.83	1.01	0.50	0.65	0.89	0.30	0.55
FHC(56)	0.80	....	....	....	....	....	....
FAO(57)	0.00	0.15	0.34	0.07	0.06	0.08	0.08
FAI(58)	0.67	1.23	0.55	0.62	0.15	0.05	0.20
FAC(59)	0.00	....	....	....	....	....	....
FKO(60)	0.32	0.79	0.65	0.44	0.55	0.62	0.75
FKI(61)	2.26	1.64	1.49	1.21	1.00	0.98	0.87
FKC(62)	1.44	1.85	1.92	1.37	1.19	1.01	0.82
YYY(63)	0.00	0.03	0.04	0.05	0.06	0.08	0.10
ZZZ(64)	0.00	....	....	....	....	....	....

differences is a factor of 2. Alternatively, the maximum flare rate over the next several days typically differs from the persistence rate by 0.1 flares per day, or in more extreme cases by 0.6 flares per days.

We note, however, that the most extreme differences between these statistics and persistence predictions generally occur for rarely observed classes. These differences may be an artifact of poor statistics for these classes. This would suggest that merging these rare classes with similar classes may improve the ability to acurately predict flares from these regions.

4.3 ILLEGAL AND RARE CLASSES

Analysis of the data pointed to several types of infrequent errors in the reported active region classes. The most common type of error were illegal classes. In these cases, summarized in Table 3, two of the parameters disagreed about either the existence of penumbra or the polarity of the region. These illegal classes occurred 201 times, which is only 0.6% of all of the reported classes.

Table 3. Incompatible Class Parameters

Parameter	Unipolar	Bipolar	No Penumbra	Penumbra
first	A, H	B, C, D, E, F	A, B	H, C, D, E, F
second			X	R, S, H, A, K
third	X	O, I, C		I, C

The second type of classification errors were two classes, CKC and CSC, that were not clearly illegal based on the early definitions of these classes (McIntosh 1986 and the guidelines for observers in the Air Weather Service Pamphlet 105–60). The classes are now listed as illegal in the classification paper of McIntosh (1989), probably because it is somewhat contradictory to require penumbra on spots in the middle and at only one end of the region. We have treated the four occurrences of these two classes as illegal, and did not process these reports.

A third type of error were classes in which one or more of the three classification parameters were missing. Of these, there were 22 cases that could not be completed from the existing parameters. The incomplete classes could be resolved from the two existing parameters, using the criteria in Table 3. These classes were corrected to the full three-parameter class (see Table 4), and the analysis of these regions continued as normal.

Table 4. Resolution of Incomplete Classes

Reported	Complete
AX_	AXX
B_O	BXO
B_I	BXI
HR_	HRX
HS_	HSX
HH_	HHX
HA_	HAX
HK_	HKX

A fourth type of error, which is less easily recognized is the improper assignment of a region to a legal class. These improper classifications can occur due to poor seeing or observing conditions, foreshortening of regions on the limb, and human error (for further discussion see McIntosh 1989). Because the forecaster must make predictions based on data that may contain these errors, we felt it best to calculate our statistics on this "noisy" data. Therefore we have not attempted to identify these errors.

Twelve classes did not occur in the SESC-average of the 1981–1986 data (see rows and columns of periods in Table 1). We searched the entire original data set for the number of occurrences of these twelve classes. This extended data set included all of 1971 through 1986, and was not limited to the smaller sample considered in the rest of this paper. These classes are listed in Table 5 in a way to suggest combinations of parameters that should possibly be considered illegal. One such combination has FR for the first two parameters, which requires a large penumbra for the major spot and only rudimentary penumbra for the interior spots. Another set of combinations have RC, SC, or HC as the last two parameters, which requires either rudimentary or small, symmetric, mature penumbra for the major spot and mature penumbra for the interior spots. We note that the RC combination is now considered illegal by McIntosh (1989), although no detailed reasons were presented. We suggest that these different combinations, along with possibly class FAC, may indicate a conflict about the degree of complexity and development of the region.

Table 5. Rare classes and number of occurrences in 1971–1986

FRO	4	DRC	1	DSC	14	DHC	12	FAC	7
FRI	2	ERC	0	ESC	1	EHC	5		
	FRC	0		FSC	0	FHC	3		

Because of the rarity of these classes, a single improperly assigned classification or improperly assigned region responsible for the flare could increase the average number of M flares by up to 0.5 flares per day. Merging these rare classes with similar classes would reduce the formal errors. If the classes are sufficiently similar that they could easily be confused, or might rapidly evolved from one to the other, then such a merger would not introduce new errors into the flare rate of the more frequent class.

5. CONCLUSIONS

We have presented the initial results of the newly-developed analysis software, TELSAR. This software has been applied to 5 years of active region classifications to derive statistics on the frequency of transition between classes and the subsequent rate of flaring expected from the region for the next 2–7 days. These tabulated statistics form the first study of this kind that we are aware of. It is hoped that these results can be used to improve flare forecasts on the intermediate timescale of several days.

The most frequent transitions between classes involve single-step changes in only one of the three classification parameters. The reverse of these transitions were also very frequent, suggesting that the regions either oscillate in class due to observational error, or traversed the same sequence forwards and then backwards as the region grows and then decays. This could be tested with temporally averaged classes. In addition, such averages may reduce the number of entries in the transition matrix by reducing the frequency of rarely observed, spurious transitions.

The maximum future flare rate differs from persistence predictions by up to 0.5 M flares per day, with 0.1 being a more typical difference. These initial results suggest that evolutionary statistics can be used to improve intermediate term flare forecasts, but their significance has not yet been tested. One such test would compare the number of flares actually produced by the region several days later with the TELSAR-derived, expected rate. Another test would determine the difference between the TELSAR-derived future rates and the persistence rates. This could be done through an analysis of the propagation of errors, starting with the statistical errors on the average number of flares observed per day for each class. The resulting errors on the TELSAR-derived flare rates should exceed the difference with persistence rates for the evolutionary statistics to prove valuable.

The frequency of observation of several classes was very low, often less frequent than reports of illegal classes. This suggests that reduction in the number of allowed classes should be considered. Such a reduction may improve the flare statistics and thereby improve flare forecasts.

6. ACKNOWLEDGEMENTS

7. REFERENCES

Bray, R. J. and Loughhead, R. E., *Sunspots*, New York, Dover, 1964.
Kiepenheuer, K. O., in *The Sun*, Kuiper, G. P. (ed), p. 322, Univ. Chicago, 1953.
Kildahl, K. J. N., Frequency of Class M and X Flares by Sunspot Class (1969–1976), in *Solar-Terrestrial Predictions Proceedings*, vol. 3, Donnelly, R. (ed), p. 166, 1980.
McIntosh, P. S., The Classification of Sunspot Groups, *Solar Physics*, in press, 1989,.
McIntosh, P. S., Flare Forecasting Based on Sunspot Classification, in *Solar-Terrestrial Predictions*, Simon, P. A., Heckman, G., and Shea, M. A. (eds), p. 357, 1986.
McIntosh, P. S., The Birth and Evolution of Sunspots: Observations, in *The Physics of Sunspots*, Cram, L. E., and Thomas, J. H. (eds), p. 7, 1981.
Waldmeier, M., *Ergebnisse und Probleme den Sonnenforschung*, 2nd ed., Leipzig, Geest u. Protig, 1955.

REPORT DOCUMENTATION PAGE

[standard form instructional text, illegible]

2. REPORT DATE	3. REPORT TYPE AND DATES COVERED
20 December 1989	Reprint

4. TITLE AND SUBTITLE

A Study of the Evolution of Solar Active Regions for Improving Solar Flare Forecasts

5. FUNDING NUMBERS

PE: 61102F
PR 2311 — TA G5 — WU AB

Project Order:
GLH7-6022

6. AUTHOR(S)

Patricia L. Bornmann; Darren Kalmbach*; David Kulhanek*; April Casale*

7. PERFORMING ORGANIZATION NAME(S) AND ADDRESS(ES)

Cooperative Institute for Research in Environmental Sciences
NOAA Space Environment Laboratory
325 Broadway
Boulder, CO 80303

8. PERFORMING ORGANIZATION REPORT NUMBER

9. SPONSORING/MONITORING AGENCY NAME(S) AND ADDRESS(ES)

Geophysics Laboratory
Hanscom AFB
Massachusetts 01731-5000

Contract Manager: Frederick Rich/PHG

10. SPONSORING/MONITORING AGENCY REPORT NUMBER

GL-TR-89-0337

11. SUPPLEMENTARY NOTES * Computer Science Dept, University of Colorado, Boulder, CO 80309

Proceedings of the Solar-Terrestrial Predictions Workshop, 16-20 Oct 1989, Leura, Australia

12a. DISTRIBUTION AVAILABILITY STATEMENT

APPROVED FOR PUBLIC RELEASE; DISTRIBUTION UNLIMITED

12b. DISTRIBUTION CODE

13. ABSTRACT (Maximum 200 words)

Statistics on the frequency of transition between active region classes were calculated and used to derive the expected rate of flaring for the next 2-7 days. Five years of McIntosh active region classifications were analyzed using the newly-developed software called TELSAR (Tracking and EvoLution of Solar Active Regions). The most frequent transitions between these 63 different classes usually involve a single-step change in one of the three classification parameters. The evolution of the classes and the average, single-day flare rate were used to predict flare rates for each class over the next several days. For flares of X-ray class M (peak 1-8 Å flux between 10^{-5} and 10^{-4} W m^{-2}), these rates can differ from persistence predictions by more than 0.5 flares per day, although a more typical difference is 0.1 flares per day. The rarity of some classes suggests that merging these classes with others may improve flare statistics and thereby improve flare forecasts.

14. SUBJECT TERMS

Solar flares
Solar activity
Solar active regions
X-ray flares
Flare forecasts

15. NUMBER OF PAGES

8

16. PRICE CODE

17. SECURITY CLASSIFICATION OF REPORT	18. SECURITY CLASSIFICATION OF THIS PAGE	19. SECURITY CLASSIFICATION OF ABSTRACT	20. LIMITATION OF ABSTRACT
Unclassified	Unclassified	Unclassified	SAR

90 01 02 048